2016 American Control Conference (ACC)
Boston Marriott Copley Place
July 6-8, 2016. Boston, MA, USA

Adaptive Control of Mass-Spring Systems with Unknown Hysteretic Contact Friction

Mohammad Al Janaideh and Dennis Bernstein

***Abstract*— We apply retrospective cost adaptive control (RCAC) to a command-following problem for mass-spring systems with unknown contact friction. Dahl, LuGre, and Maxwell-slip models are used to generate the friction force. We consider a single-degree-of-freedom oscillator with control force applied directly to the mass, as well as a noncolocated two-degree-of-freedom oscillator with control force applied to the secondary mass and performance given by the position of the primary mass. For harmonic command following, we show that RCAC achieves internal model control without knowledge of either the friction force or the friction model.**

I. Introduction

Virtually all mechanical systems are affected by friction [1, 2]. In motion control applications, friction degrades performance and, for multiple reasons, may present a significant challenge. In particular, friction can vary over time due to changes in surface properties and lubrication; it may depend on loads and geometry; it may be difficult to model and thus is usually uncertain; it is difficult to measure or estimate; and it is highly nonlinear and hysteretic [3–8].

In view of these challenges, it is not surprising that a wide variety of feedback control techniques have been used to compensate for friction, including both fixed-gain [9, 10] and adaptive methods [11–16]. The present paper takes the latter approach by applying retrospective cost adaptive control (RCAC) to illustrative systems [17–19].

In the present paper, we consider a single-degree-of-freedom oscillator with control force applied to the mass, as well as a two-degree-of-freedom oscillator with the control force applied to the secondary mass and the performance given by the position of the primary mass. The challenging aspect of these examples is the fact that all of the masses are subjected to friction, where the friction model is unknown and no direct measurement of the friction force available.

To generate the friction force, we consider three friction models, namely, the Dahl [20], LuGre [8], and Maxwell-slip models [21, 22]. The contribution of the present paper is thus a numerical investigation of the performance of RCAC without knowledge of either the friction force or the underlying friction model. As a performance metric, we use phase shift calculations to determine whether RCAC achieves internal model control with harmonic command following. This method was used in [23] for Hammerstein systems. However, the applications in the present paper are not Hammerstein systems. We stress that the phase-shift calculations are for analysis only; all of the closed-loop simulations are based on nonlinear friction models.

M. Al Janaideh is with the Department of Mechanical and Industrial Engineering, University of Toronto, Toronto, ON M5S 3G8, Canada.

D. S. Bernstein is with the Department of Aerospace Engineering, The University of Michigan, Ann Arbor, MI 48109, USA.

II. Friction Models

We consider the mass-spring system shown in Figure 1(a), where $q(t)$ denotes the mass position. With $x_1 \triangleq q$ and $x_2 \triangleq \dot{q}$, it follows that

$$\dot{x}_1(t) = x_2(t), \tag{1}$$

$$\dot{x}_2(t) = -\frac{C}{M}x_2(t) - \frac{K}{M}x_1(t) + \frac{F(t)}{M} - \frac{F_{\mathrm{f}}(t)}{M}, \tag{2}$$

$$y(t) = x_1(t), \tag{3}$$

where $y(t)$ is the position measurement available to the controller, $F(t)$ is the control force, and $F_{\mathrm{f}}(t)$ is the friction force. Equations (1)-(3) can be expressed as

$$\dot{x}(t) = A_{\mathrm{c}}x(t) + B_{\mathrm{c}}[F(t) - F_{\mathrm{f}}(t)], \tag{4}$$

$$y(t) = C_{\mathrm{c}}x(t), \tag{5}$$

where $A_{\mathrm{c}} \triangleq \begin{bmatrix} 0 & 1 \\ -\frac{K}{M} & -\frac{C}{M} \end{bmatrix}$, $B_{\mathrm{c}} \triangleq \begin{bmatrix} 0 \\ \frac{1}{M} \end{bmatrix}$, and $C_{\mathrm{c}} \triangleq \begin{bmatrix} 1 & 0 \end{bmatrix}$. We now review the Dahl, LuGre, and Maxwell-slip friction models used to generate the friction force $F_{\mathrm{f}}(t)$.

A. Dahl friction model

The Dahl friction model is given by

$$\dot{F}_{\mathrm{f}}(t) = \sigma\Big|1 - \frac{F_{\mathrm{f}}(t)}{f_{\mathrm{C}}}\dot{q}(t)\Big|^{\varepsilon}\operatorname{sgn}\Big(1 - \frac{F_{\mathrm{f}}(t)}{f_{\mathrm{C}}}\dot{q}(t)\Big)\dot{q}(t), \tag{6}$$

where $\sigma > 0$ represents the slope of force-deflection curve for $F_{\mathrm{f}} = 0$, f_{C} is the Coulomb friction force, and $\varepsilon > 0$ influences the shape of the hysteresis loop. For all $\varepsilon \geq 1$, the Dahl model is a Lipschitz-continuous, rate-independent hysteresis model [8]. We consider the Dahl model with $\varepsilon = 1$, $\sigma = 0.75$, and $f_{\mathrm{C}} = 1$ N.

B. LuGre friction model

The LuGre model [8], which models the asperities of two surfaces as elastic bristles, is given by

$$\dot{m}(t) = \dot{q}(t) - \frac{|\dot{q}(t)|}{\rho(\dot{q}(t))}m(t), \tag{7}$$

$$F_{\mathrm{f}}(t) = \sigma_1 m(t) + \sigma_2\dot{m}(t) + \sigma_3\dot{q}(t), \tag{8}$$

where

$$\rho(\dot{q}(t)) \triangleq \frac{f_{\mathrm{C}}}{\sigma_1} + \frac{f_{\mathrm{s}} - f_{\mathrm{C}}}{\sigma_1}e^{-(\frac{\dot{q}(t)}{v_{\mathrm{s}}})^2}, \tag{9}$$

where $m(t)$ is the average deflection of the bristles, $\sigma_1 > 0$, $\sigma_2 > 0$, and $\sigma_3 > 0$ represent stiffness, damping, and

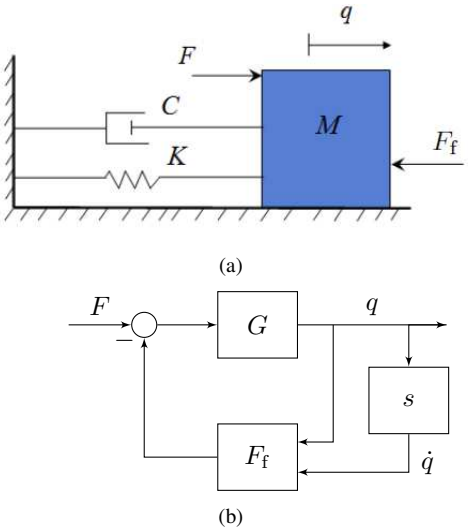

Fig. 1. (a) Force-actuated mass-spring system, where F_f is the unknown friction force and F is the external input force. (b) Force-actuated mass-spring system, where $G(s) = \frac{1}{Ms^2+Cs+K}$, $q(t)$ is the output displacement, F is the external force, and F_f is the friction force.

mass, respectively, f_s is the stiction force, and v_s is the Stribeck velocity, which is the velocity at which the steady-state friction force starts decreasing. The LuGre model is a Lipschitz-continuous, rate-dependent hysteresis model [8]. We consider the LuGre model of $\sigma_1 = 10^5$ N/m, $\sigma_2 = \sqrt{10^5}$ N-s/m, $\sigma_3 = 0.4$ N-s/m, v_s = 0.001 m/s, $f_\mathrm{s} = 1.5$ N, and $f_\mathrm{c} = 1$ N.

C. Maxwell-slip model

The Maxwell-slip model with deadband width $\Delta_i \in \mathbb{R}$ for $i = 1, \ldots, N$ [21, 22] is given by

$$F_\mathrm{f}(t) = \sum_{i=1}^{N} \lambda_i \big(q(t) - q_i(t)\big), \tag{10}$$

$$\dot{q}_i = \begin{bmatrix} \mathcal{M}(q_i(t), \dot{q}(t), \Delta_i) & 1 - \mathcal{N}(q_i(t), \dot{q}(t), \Delta_i) \end{bmatrix} \begin{bmatrix} \ddot{q}_+(t) \\ \ddot{q}_-(t) \end{bmatrix}, \tag{11}$$

where $\mathcal{M}(q_i, q, \Delta) \triangleq \mathcal{U}(-q_i + q - \Delta_i)$, $\mathcal{N}(q_i, q, \Delta) \triangleq \mathcal{U}(-q_i + q + \Delta_i)$, and

$$\mathcal{U}(x) = \begin{cases} 1, & x \geq 0, \\ 0, & x < 0. \end{cases}$$

The Maxwell-slip model is a discontinuous rate-independent hysteresis model [8]. We consider the Maxwell-slip model with $N = 4$, $\lambda_1 = 1$, $\lambda_2 = 0.3$, $\lambda_3 = 0.1$, $\lambda_4 = 0.4$, $\Delta_1 = 0.5$, $\Delta_2 = 1$, $\Delta_3 = 0.5$, and $\Delta_4 = 0.5$.

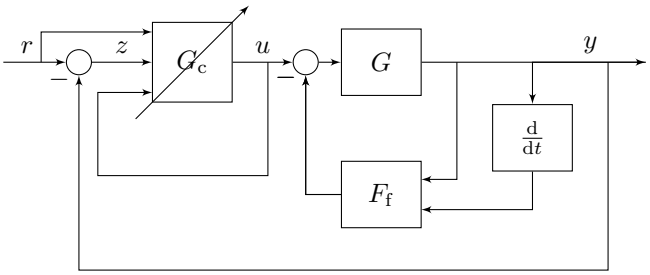

Fig. 2. Command-following problem for the force-actuated mass-spring system with retrospective cost adaptive control update of the controller $G_\mathrm{c}(s)$.

III. Adaptive Control of the Force-Actuated Mass-Spring System with Friction Nonlinearity

A. Problem formulation

For sampled-data control, let h be the sampling time and $k = 0, 1, 2, \ldots$. To discretize (5) and (6), consider

$$x(hk + h) - x(hk) \cong hA_\mathrm{c}x(hk) + hB_\mathrm{c}[u(hk) - F_\mathrm{f}(hk)], \tag{12}$$

$$y(hk) = C_\mathrm{c}x(hk), \tag{13}$$

where $u = F$ represents the control force. Then

$$x(k+1) \cong Ax(k) + B[u(k) - F_\mathrm{f}(k)], \tag{14}$$

where

$$A \triangleq I_2 + hA_\mathrm{c}, \quad B \triangleq hB_\mathrm{c}, \tag{15}$$

and, for convenience $x(k)$ denotes $x(kh)$. We use (15) to discretize (1)-(3) as

$$x(k+1) = Ax(k) + B[u(k) - F_\mathrm{f}(k)], \tag{16}$$

$$y(k) = Cx(k), \tag{17}$$

where $A \triangleq \begin{bmatrix} 1 & h \\ -\frac{Kh}{M} & 1 - \frac{Ch}{M} \end{bmatrix}$, $B \triangleq \begin{bmatrix} 0 \\ \frac{1}{M} \end{bmatrix}$, $C \triangleq \begin{bmatrix} 1 & 0 \end{bmatrix}$, and

$$z(k) \triangleq r(k) - y(k), \tag{18}$$

where $z(k)$ is the command-following error and $r(k)$ is the position command. The goal is to determine u that makes z small.

B. RCAC

A block diagram for (17)-(20) with RCAC is shown in Figure 2. We assume that the discrete-time transfer function G that relates the control force to the displacement of the mass is unknown except for an estimate of a single nonzero Markov parameter as needed for RCAC. The friction model and friction force are also unknown.

The adaptive controller has the form

$$u(k) = \sum_{i=1}^{n_\mathrm{c}} M_i(k)u(k-i) + \sum_{i=1}^{n_\mathrm{c}} N_i(k)z(k-i) + \sum_{i=1}^{n_\mathrm{c}} Q_i(k)r(k-i), \tag{19}$$

where, for all $i = 1, \ldots, n_c$, $M_i(k) \in \mathbb{R}$, $N_i(k) \in \mathbb{R}$, and $Q_i(k) \in \mathbb{R}$. The control (19) can be expressed as

$$u(k) = \theta(k)\phi(k-1),$$

where

$$\theta(k) \triangleq \begin{bmatrix} M_1(k) & \cdots & M_{n_c}(k) & N_1(k) & \cdots & N_{n_c}(k) & Q_1(k) & \cdots & Q_{n_c}(k) \end{bmatrix} \in \mathbb{R}^{1\times 3n_c}$$

and

$$\phi(k-1) \triangleq \begin{bmatrix} u(k-1) & \cdots & u(k-n_c) & z(k-1) & \cdots & z(k-n_c) & r(k-1) & \cdots & r(k-n_c) \end{bmatrix}^{\mathrm{T}} \in \mathbb{R}^{3n_c}.$$

Next, define the cumulative cost function

$$J_{\mathrm{R}}(\theta, k) \triangleq \sum_{i=2}^{k} \|\phi^{\mathrm{T}}(i-2)\theta^{\mathrm{T}}(k) - \hat{U}^{\mathrm{T}}(i-1)\|^2 + (\theta(k)-\theta_0)P_0^{-1}(\theta(k)-\theta_0)^{\mathrm{T}}, \tag{20}$$

where $\|\cdot\|$ is the Euclidean norm. Minimizing (20) yields

$$\begin{aligned}\theta^{\mathrm{T}}(k) = \theta^{\mathrm{T}}(k-1) &+ P(k-1)\phi(k-2) \\ &\cdot [\phi^{\mathrm{T}}(k-1)P(k-1)\phi(k-2)+1]^{-1} \\ &\cdot [\phi^{\mathrm{T}}(k-2)\theta^{\mathrm{T}}(k-1) - \hat{U}^{\mathrm{T}}(k-1)],\end{aligned} \tag{21}$$

The error covariance is updated by

$$\begin{aligned}P(k) = P(k-1) &- P(k-1)\phi(k-2) \\ &\cdot [\phi^{\mathrm{T}}(k-2)P(k-1)\phi(k-1)+1]^{-1} \\ &\cdot \phi^{\mathrm{T}}(k-2)P(k-1).\end{aligned} \tag{22}$$

We initialize the error covariance matrix as $P_0 = \alpha I_{3n_c}$, where $\alpha > 0$.

IV. Performance Analysis

Consider the force-actuated mass-spring system shown in Fig. 2 with the harmonic command $r(k) = \mathrm{Re}\{A_r e^{(\jmath\Omega k)}\}$, where A_r is a complex number and Ω is the command frequency. Since the input is harmonic, the friction force is harmonic. For analysis only, we consider the main harmonic component in the friction force for the phase-shift calculations. Then a transfer function G_{F} that represents the main harmonic component in the friction force can be used to represent the friction force F_{f}. Then the system shown in Fig. 2 with the controller can be represented as in Fig. 3, where

$$G_{ur} \triangleq \frac{G_{\mathrm{c}}}{1 + G_{\mathrm{c}}G_{uy}}, \tag{23}$$

and

$$G_{uy} \triangleq \frac{G}{1 + G_{\mathrm{c}}G + G_{\mathrm{F}}G}. \tag{24}$$

If u is also harmonic, then

$$u(k) = \mathrm{Re}\{A_r |G_{ur}(e^{\jmath\Omega})| e^{\jmath(\Omega k + \angle G_{ur}(e^{\jmath\Omega}))}\}, \tag{25}$$

where $|G_{ur}(e^{\jmath\Omega})|$ and $\angle G_{ur}(e^{\jmath\Omega})$ are, respectively, the magnitude and phase of G_{ur}, at the frequency Ω. Then the harmonic steady-state response is given by

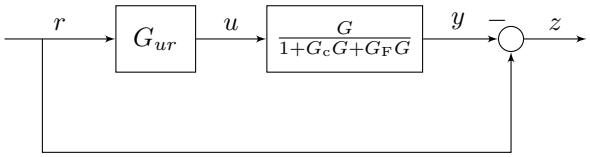

Fig. 3. Linearized approximation for the force-actuated mass-spring system with RCAC adaptive control. The friction force F_{f} is approximated by the transfer function G_{F}.

$$y(k) = \mathrm{Re}\{A_r |G_{ur}(e^{\jmath\Omega})||G_{uy}(e^{\jmath\Omega})| \tag{26}$$

$$e^{\jmath(\Omega k + \angle G_{ur}(e^{\jmath\Omega}) + \angle G_{uy}(e^{\jmath\Omega}))}\}. \tag{27}$$

Thus

$$z(k) = \mathrm{Re}\{A_r e^{(\jmath\Omega k)}\} - \mathrm{Re}\{A_r |G_{ur}(e^{\jmath\Omega})||G_{uy}(e^{\jmath\Omega})| e^{\jmath(\Omega k + \angle G_{ur}(e^{\jmath\Omega}) + \angle G_{uy}(e^{\jmath\Omega}))}\}. \tag{28}$$

Therefore, $z(k) = 0$ if and only if the magnitude and phase of $G_{ur}(e^{\jmath\Omega})$ satisfy

$$|G_{ur}(e^{\jmath\Omega})| = \frac{1}{|G_{uy}(e^{\jmath\Omega})|}, \tag{29}$$

$$\angle G_{ur}(e^{\jmath\Omega}) = -\angle G_{uy}(e^{\jmath\Omega}). \tag{30}$$

In the following examples, we use the Fourier transform to determine the most significant frequency component in the output y. Then, we calculate $\angle G_{uy}(e^{\jmath\Omega})$, which is the phase between the control force u and output y. Then, we compare $\angle G_{uy}(e^{\jmath\Omega})$ with $\angle G_{ur}(e^{\jmath\Omega})$, which represents the phase between the command r and the control force u. In order to verify (28) and (29), we approximate F_{f} by the transfer function G_{F} to obtain the phase of $\angle G_{uy}(e^{\jmath\Omega})$. This provides a technique for determining whether RCAC develops an internal model of the harmonic command.

V. SDOF Oscillator

We now consider (16)-(18) with $h = 0.001$ sec. Consider (16)-(18) with the magnitude and phase shift of the most significant harmonic component in the command $r(k)$, control signal $u(k)$, and mass position $q(k)$ to determine whether RCAC achieves internal model control.

Example 5.1: Consider the command $r(k) = 5\sin(\frac{\pi}{10}hk)$ with the Dahl model, and let $M = 1$ kg, $C = 2$ N-s/m, and $K = 1$ N/m. We use RCAC with $n_c = 20$ and $\alpha = 0.1$. Figure 4 shows that RCAC drives the command-following error z to zero. Figure 4 shows that the phase shift between the command $r(k)$ and the control $u(k)$ is -7.007 deg, and the phase shift between the control signal $u(k)$ and the mass position $q(k)$ is 7.087 deg. Thus RCAC achieves the correct gain and phase shift that stabilize the mass-spring system with unknown friction force at the command frequency. ■

Example 5.2: Consider the command $r(k) = 5\sin(\frac{\pi}{10}hk)$ with the LuGre model (8)-(10), and let

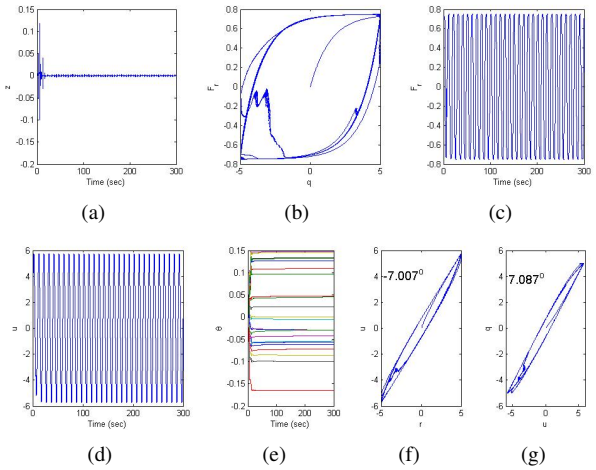

Fig. 4. Example 5.1: (a) shows the command-following error z with the Dahl model whose input and output are shown in (b) for the closed-loop system with RCAC, (c) shows the friction force, (d) shows the control u, (e) shows the evolution of the controller coefficients θ, (f) shows the relationship between the command r and the control u, and (g) shows the relationship between the control u and the mass position q.

$M = 1$ kg, $C = 2$ N-s/m, and $K = 1$ N/m. Then $\omega_{\rm n} = 1$ rad/sec, $\zeta = 1$, and $G(z) = \frac{0.2642z+0.1353}{z^2-0.7358z+0.1353}$. We use RCAC with $n_{\rm c} = 20$ and $\alpha = 0.01$. Figure 5 shows that RCAC drives the command-following error z to zero. Figure 5 shows that the phase shift between the command input $r(k)$ and the control signal $u(k)$ is -12.381 deg, and the phase shift between the control signal $u(k)$ and the mass position $q(k)$ is 12.407 deg. Thus RCAC achieves the correct gain and phase shift that stabilize the mass-spring system with unknown friction force at the command frequency. ■

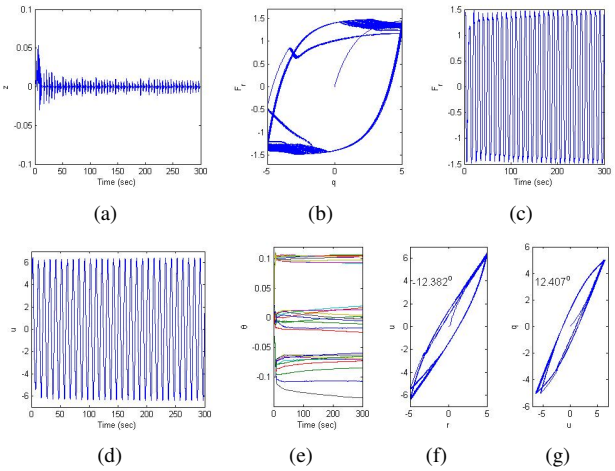

Fig. 5. Example 5.2: (a) shows the command-following error z with the LuGre model whose input and output are shown in (b) for the closed-loop system with RCAC, (c) shows the friction force, (d) shows the control u, (e) shows the evolution of the controller coefficients θ, (f) shows the relationship between the command signal r and the control signal u, and (g) shows the relationship between the control u and the mass position q.

Example 5.3: Consider the command $r(k) = 5\sin(\frac{\pi}{10}hk)$ with the Maxwell-slip model (11) and

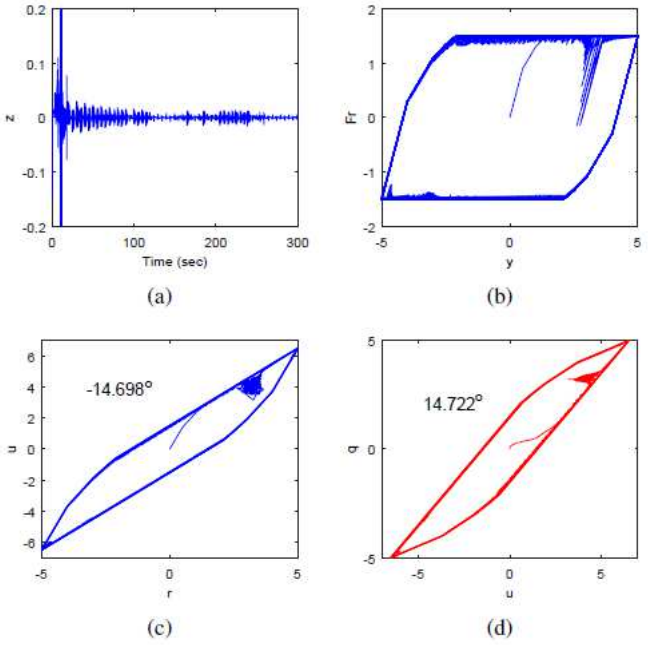

Fig. 6. Example 5.3: (a) shows the command-following error z with the Maxwell-slip model whose input and output are shown in (b) for the closed-loop system with RCAC, (c) shows the relationship between the command signal r and the control u, and (d) shows the relationship between the control u and the mass position q.

(12), and let $M = 1$ kg, $C = 1$ N-s/m, and $K = 1$ N/m. We use RCAC with $n_{\rm c} = 8$ and $\alpha = 0.01$. Figure 6 shows that RCAC drives the command-following error z to zero. Figure 4 shows that the phase shift between the command input $r(k)$ and the control signal $u(k)$ is -14.698 deg, and the phase shift between the control signal $u(k)$ and the mass position $q(k)$ is 14.722 deg. Thus RCAC achieves the correct gain and phase shift that stabilize the mass-spring system with unknown friction force at the command frequency. ■

Example 5.4: Consider Examples 5.1 and 5.2 with $M = 1$ kg, $C = 1$ N-s/m, and $K = 2$ N/m. Then $\omega_{\rm n} = 1.414$ rad/sec, $\zeta = 0.3536$, and $G(z) = \frac{0.3145z+0.2206}{z^2-0.2977z+0.3679}$. We use RCAC with $n_{\rm c} = 20$ and $\alpha = 0.1$. Figure 7 shows that RCAC drives the command-following error z to zero. ■

VI. Two-degree-of-freedom oscillator

As shown in Figure 8, we consider a two-degree-of-freedom oscillator with force applied to the mass M_2 with performance given by the position of the mass M_1. The friction forces $F_{\rm f1}$ and $F_{\rm f2}$ applied to M_1 and M_2 are unknown, and the external force F is applied to mass M_1. Let q_1 denote the position of mass M_1, and q_2 the position of mass M_2. We consider

$$x(k+1) = Ax(k) + B\begin{bmatrix} \frac{F(k)}{M_1} - \frac{F_{\rm f1}(k)}{M_1} \\ -\frac{F_{\rm f2}(k)}{M_2} \end{bmatrix}, \tag{31}$$

$$y(k) = Cx(k), \tag{32}$$

where $x^{\rm T} = \begin{bmatrix} x_1 & x_2 & x_3 & x_4 \end{bmatrix}$, where $x_1(k) = q_1(k)$, $x_3(k) = q_2(k)$, $x_2(k)$ and $x_4(k)$ are the velocities of M_1

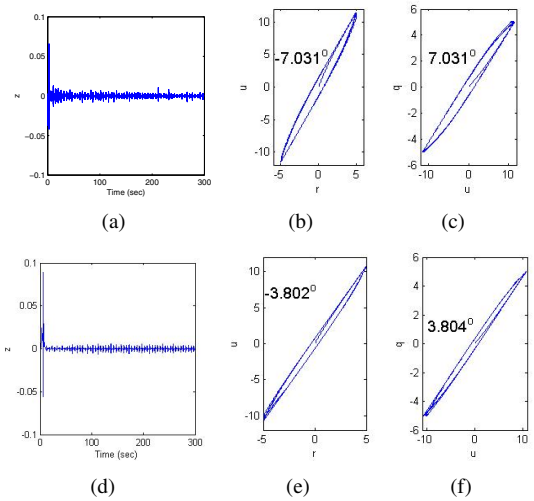

Fig. 7. Example 5.4: (a) shows the command-following error z with the LuGre model whose input and output are shown in (b) for the closed-loop system with RCAC, (b) shows the relationship between the command r and the control u, (c) shows the relationship between the control u the mass position q, (d) shows the command-following error z with the Dahl model whose input and output are shown in (b) for the closed-loop system with RCAC, (e) shows the relationship between the command signal r and the control u, and (f) shows the relationship between the control u and the mass position q.

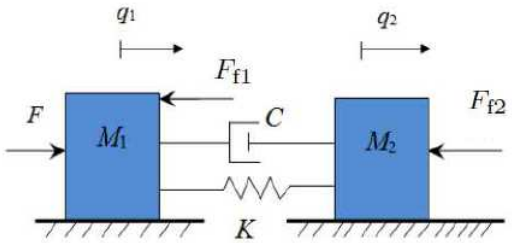

Fig. 8. Force-actuated mass-spring system, where F is the external force, F_{f1} and F_{f2} are unknown friction forces, F is the external force, q_1 is the position of the secondary mass M_1, and q_2 is the position of the primary mass M_2. The performance variable is the command-following error for M_2.

and M_2, respectively. Then

$$A = \begin{bmatrix} 1 & h & 0 & 0 \\ -\frac{hK}{M_1} & 1-\frac{hC}{M_1} & \frac{hk}{M_1} & -\frac{hC}{M_1} \\ 0 & 0 & 1 & h \\ \frac{hK}{M_2} & \frac{hC}{M_2} & -\frac{hk}{M_2} & 1 \end{bmatrix}, \quad B = \begin{bmatrix} 0 & 0 \\ 1 & 0 \\ 0 & 0 \\ 0 & 1 \end{bmatrix},$$

$$C = \begin{bmatrix} 1 & 0 & 0 & 0 \\ 0 & 0 & 1 & 0 \end{bmatrix},$$

$$z(k) = r(k) - q_2(k). \tag{33}$$

The control force u is given by

$$u(k) = \sum_{i=1}^{n_c} M_i(k)u(k-i) + \sum_{i=1}^{n_c} N_i(k)z(k-i) + \sum_{i=1}^{n_c} Q_i(k)q_1(k-i). \tag{34}$$

A. Numerical examples: two-degree-of-freedom oscillator

All of the examples in this section consider (30)-(33) with $h = 0.001$ sec.

Example 6.1: We consider the command $r(k) = 3\sin(4\frac{\pi}{10}kh) + 2\sin(6\frac{\pi}{10}kh)$ with LuGre model with $\sigma_3 = 0.4$ N-s/m for the friction force F_{f1}. We consider F_{f2} with the LuGre model with $\sigma_3 = 1$N-s/m. Let $M_1 = M_2 = 1$ kg, $C = 1$ N-m/s, and $K = 1$ N/m. We use RCAC with $n_c = 5$ and $\alpha = 1$. Figure 9 shows the command-following error z, the friction forces F_{f1} and F_{f2}, and the control signal $u(k)$. ■

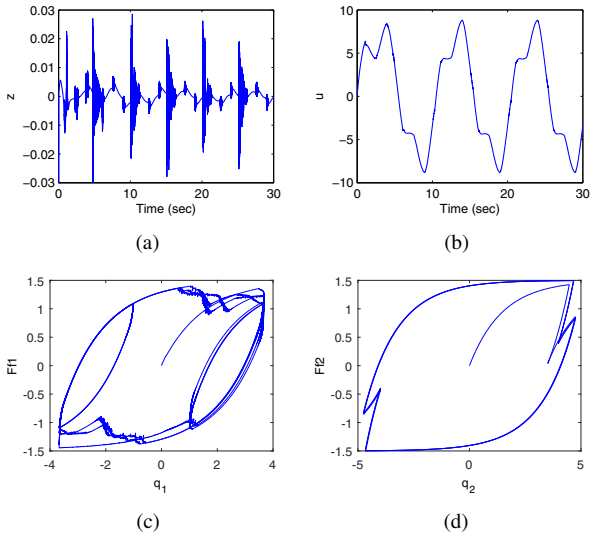

Fig. 9. Example 6.1: (a) shows the error z. The friction forces F_{f1} and F_{f2} shown in (c) and (d), respectively. (b) shows the control u.

Example 6.2: We consider the command $r(k) = 3\sin(4\frac{\pi}{10}kh) + 2\sin(6\frac{\pi}{10}kh)$ with the LuGre model of Example 5.2 and Maxwell model of Example 5.3. Let $M_1 = M_2 = 1$ kg, $C = 1$ N-m/s, and $K = 1$ N/m. We use RCAC with $n_c = 5$ and $\alpha = 1$. Figure 10 shows the command-following error z, the friction forces F_{f1} and F_{f2}, and the control signal $u(k)$. ■

These examples show that RCAC can stabilize the closed-loop system consisting of a two-degree-of-freedom oscillator with unknown friction forces produced by an unknown friction model.

VII. Conclusions

Retrospective cost adaptive control (RCAC) was applied to a command-following problem involving a single-degree-of-freedom oscillator with control force applied to the mass, as well as a two-degree-of-freedom oscillator with force applied to the secondary mass, measurements of the positions of both masses, and performance given by the position error of the primary mass. The friction forces characterized by the Dahl, LuGre, and Maxwell-slip hysteresis models are unknown. RCAC drives the command-following error of the closed-loop system to zero. The numerical results in the paper show that RCAC achieves internal model control. Future work will

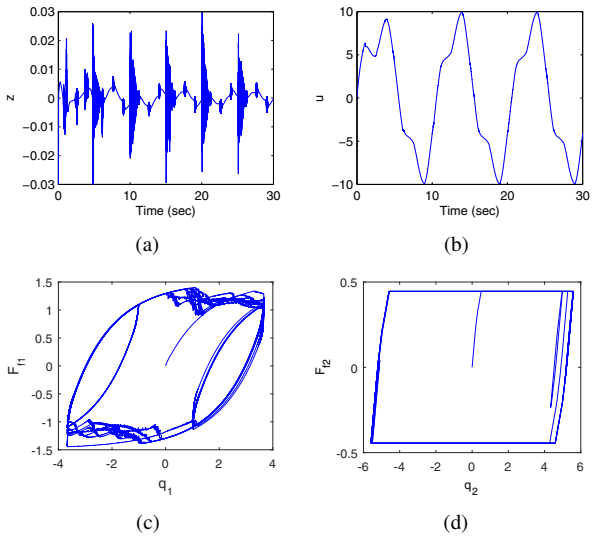

Fig. 10. Example 6.2: (a) shows the error z. The friction forces F_{f1} and F_{f2} are shown in (c) and (d), respectively. (b) shows the control u.

consider the more challenging case for the two-degree-of-freedom oscillator where only the position of the primary mass is measured.

REFERENCES

[1] B. Armstrong-Helouvry, *Control of Machines with Friction*, Boston, MA, Kluwer, 1991.

[2] B. Armstrong-Helouvry, P. Dupont, and C. Canudas de Wit, "A survey of model, analysis tools and compensation methods for the control of machines with friction," *Automatica*, vol. 30, no. 7, pp. 1083-1138, 1994.

[3] C. Canudas de Wit, H. Olsson, K. J. Astrom, and P. Lischinsky, "A new model for control of systems with friction," *IEEE Trans. Autom. Contr.*, vol. 40, no. 3, pp. 419-425, 1995.

[4] J. Swevers, F. Al-Bender, C. Ganseman, and T. Projogo, "An integrated friction model structure with improved presliding behavior for accurate friction compensation," *IEEE Trans. Autom. Contr.*, vol. 45, no. 4, pp. 675-686, 2000.

[5] V. Lampaert, J. Swevers, and F. Al-Bender, "Modification of the Leuven integrated friction model structure," *IEEE Trans. Autom. Contr.*, vol. 47, no. 4, pp. 683-687, 2002.

[6] D. S. Bernstein, "Ivory Ghost," *IEEE Contr. Sys. Mag.*, Vol. 27, pp. 16-17, 2007.

[7] B. S. R. Armstrong and Q. Chen, "The Z-Properties Chart," *IEEE Contr. Sys. Mag.*, vol. 28, pp. 79-89, 2008.

[8] A. K. Padthe, B. Drincic, J. Oh, D. D. Rizos, S. D. Fassois, and D. S. Bernstein, "Duhem Modeling of Friction-Induced Hysteresis: Experimental Determination of Gearbox Stiction," *IEEE Contr. Sys. Mag.*, vol. 28, pp. 90-107, 2008.

[9] S. Southward, C. Radcliffe, and C. MacCluer, "Robust nonlinear stick-slip friction compensation," *J. Dyn. Sys. Meas. Contr.*, vol. 113, no. 4, pp. 639–645, 1991.

[10] J. Amin, B. Friedland, and A. Harnoy, "Implementation of a friction estimation and compensation technique,"*IEEE Contr. Sys. Mag.*, vol. 17, no. 4, pp. 71–76, 1997.

[11] S. W. Lee and J.-H. Kim, "Robust adaptive stick-slip friction compensation," *IEEE Trans. Ind. Electron.*, vol. 42, no. 5, pp. 474-479, 1995.

[12] L. Freidovich, A. Robertsson, A. Shiriaev, and R. Johansson, "LuGre-model-based friction compensation," *IEEE Trans. Contr. Sys. Tech.*, vol. 18, no. 1, pp. 194–200, 2010.

[13] L. Marton and B. Lantos, "Control of mechanical systems with Stribeck friction and backlash," *Sys. Contr. Lett.*, vol. 58, no. 2, pp. 141147, 2009.

[14] C. Canudas de Wit and P. Lischinsky, "Adaptive friction compensation with partially known dynamic friction model," *Int. J. Adapt. Contr. Sig. Proc.*, vol. 11, no. 1, pp. 65-80, 1997.

[15] Y. Tan, C. Jie, and T. Hualin, "Adaptive backstepping control and friction compensation for AC servo with inertia and load uncertainties," *IEEE Trans. Indus. Electro.*, vol. 5, no. 5, pp. 994-952, 2003.

[16] C. Canudas de Wit, K. Astrom, and K. Braun, "Adaptive friction compensation in DC-motor drives," *IEEE J. Robot. Auto.*, vol. 3, no. 6, pp. 681-685, 1987.

[17] R. Venugopal and D. S. Bernstein, "Adaptive disturbance rejection using ARMARKOV system representations," *IEEE Trans. Contr. Sys. Tech.*, vol. 8, no. 2, pp. 257-269, 2000.

[18] M. A. Santillo and D. S. Bernstein, "Adaptive control based on retrospective cost optimization," *AIAA J. Guid. Contr. Dyn.*, vol. 33, no. 2, pp. 289-304, 2010.

[19] J. B. Hoagg, M. A. Santillo and D. S. Bernstein, "Discrete-time adaptive command following and disturbance rejection for minimum-phase systems with unknown exogenous dynamics," *IEEE Trans. Autom. Contr.*, vol. 53, no. 4, pp. 912-928, 2008.

[20] P. Dahl, "Solid friction damping of mechanical vibrations," *AIAA J.*, vol. 14, no. 2, pp. 1675-1682, 1976.

[21] D. D. Rizos and S. D. Fassois, "Presliding friction identification based upon the Maxwell slip model structure," *Chaos*, vol. 14, no. 2, pp. 431–445, 2004.

[22] F. Al-Bender, V. Lampaert, and J. Swevers, "Modeling of dry sliding friction dynamics: From heuristic models to physically motivated models and back," *Chaos*, vol. 14, no. 2, pp. 446-445, 2004.

[23] M. Al Janaideh and D. S. Bernstein, "Adaptive Control of Hammerstein Systems with Unknown Prandtl-Ishlinskii Hysteresis," *Proc. Inst. Mech. Eng. I J. Syst. Contr. Eng.*, vol. 229, no. 2, pp. 149-157, 2015.